Available online at www.sciencedirect.com
SCIENCE DIRECT®
Biochemical and Biophysical Research Communications 334 (2005) 269–275
BBRC
www.elsevier.com/locate/ybbrc

Determination of the dissociation constants for recombinant c-Myc, Max, and DNA complexes: The inhibitory effect of linoleic acid on the DNA-binding step ☆

Kyung Chae Jung, Ho Sung Rhee, Chi Hoon Park, Chul-Hak Yang *

Department of Chemistry, Seoul National University, Seoul, Republic of Korea

Received 15 June 2005
Available online 27 June 2005

Abstract

c-Myc, the protein product of protooncogene *c-myc*, functions in cell proliferation, differentiation, and neoplastic disease. In this study, recombinant c-Myc and Max proteins, encompassing DNA binding (basic region) and dimerization (helix–loop–helix/leucine zipper) domain of human origin, were expressed in bacteria as Myc87 and Max85. Myc87 was purified under denatured conditions and was renatured again. The dissociation constant for the protein dimers and for dimer/DNA complexes were not detectable by isothermal titration calorimetry because of the low degree of solubility of Myc87 and Max85. Therefore, we set up equations which were used to determine the dissociation constants from the proportion of protein–DNA complexes. The dimer dissociation constants in TBS were $5.90(\pm0.54)\times10^{-7}$ M for Max85/Max85 homodimer, $6.85(\pm0.25)\times10^{-3}$ M for Myc87/Myc87 homodimer, and $2.55(\pm0.29)\times10^{-8}$ M for Myc87/Max85 heterodimer, and the DNA-binding dissociation constants in TBS were $1.33(\pm0.21)\times10^{-9}$ M for Max85/Max85/DNA, $2.27(\pm0.08)\times10^{-12}$ M for Myc87/Myc87/DNA, and $4.43(\pm0.37)\times10^{-10}$ M for Myc87/Max85/DNA. In addition, we revealed that linoleic acid which is known as an inhibitor for the formation of Max/Max/DNA complex reduced the affinity of Max homodimer for DNA. This result indicates that linoleic acid may bind to the DNA-binding region of Max homodimer.

Keywords: c-Myc; Max; Dissociation constant; Transcription factor; Electrophoretic mobility shift assay; Linoleic acid

c-Myc, the protein product of protooncogene c-*myc*, plays an important role in cell proliferation, differentiation, and neoplastic disease [1–3]. The Myc family proteins including c-, N-, and L-Myc heterodimerize with the carboxy-terminal basic/helix–loop–helix/leucine zipper (bHLHZip) domain of Max protein [4–7]. Max/Max homodimer and Myc/Max heterodimer bind with a specific DNA sequence, CACGTG (E-box) [4,8,9], but the heterodimerization and DNA binding of Max are required for transcriptional activation target genes by c-Myc as well as its ability to promote proliferation, malignant transformation, and apoptosis [1,10]. The *myc* gene is amplified in many tumors, particularly small cell-lung carcinoma, breast and cervical carcinomas [11–13]. In vitro, overexpression of Myc activates, whereas overexpression of Max represses, transcriptional activity [14]. All human tumor cells that have been examined show abnormal regulation of Myc in that removal of serum or growth factors do not cause the rapid repression of transcription and degradation of *myc* mRNA and protein characteristic of normal cells [15]. Especially in human gastric adenocarcinoma, amplified c-*myc* oncogene was found and the level of c-*myc* RNA was markedly

☆ *Abbreviations:* EMSA, electrophoretic mobility shift assay; bHLHZip, basic/helix–loop–helix/leucine zipper domain; TBS, Tris-buffered saline; PBS, phosphate-buffered saline.

* Corresponding author. Fax: +82 2 889 1568.
E-mail address: chulyang@plaza.snu.ac.kr (C.-H. Yang).

0006-291X/$ - see front matter © 2005 Elsevier Inc. All rights reserved.
doi:10.1016/j.bbrc.2005.06.088

elevated in a rapidly growing and poorly differentiated tumor, whereas it was only slightly elevated in a slowly growing and more differentiated tumor [16]. The X-ray crystal structure of Max homodimer and that of heterodimeric complexes formed with the bHLHZip region of c-Myc and Max were revealed [17,18]. Based on these analyzed structures, in vitro experiments about Max homodimer and Myc/Max heterodimer have been accelerated recently. Moreover, dissociation constants for the heterodimer formed with the recombinant bHLHZip domain of the v-Myc binding partner Max and for the v-Myc/Max/DNA complex were estimated using circular dichroism spectroscopy and quantitative electrophoretic mobility shift assay (EMSA) [19].

On the contrary, the dissociation constants for the heterodimer formed with the recombinant c-Myc/Max and for c-Myc/Max/DNA complex are not detectable by isothermal titration calorimetry (ITC) because of the low degree of solubility of recombinant c-Myc. Here, we determined the dissociation constants for the complexes formed with recombinant c-Myc and Max encompassing the dimerization and DNA-binding domain of human origin, and set up some equations which are used to determine dissociation constants by the proportion of dimer–DNA complexes. Determined dissociation constants and proposed equations serve to comprehend the data from in vitro experiments about recombinant c-Myc and Max.

Materials and methods

Construction of pET21a(+) expression vector and transformation. Recombinant *c-myc* gene and *max* gene containing DNA-binding basic domain, helix–loop–helix domain, and leucine zipper domain (kindly provided by Dr. Bruno Amati) were cloned into pET21a(+) vector. pET21a(+) carrying the N-terminal T7 promoter sequence and the C-terminal His-tag sequence is designed for use in protein overexpression and purification. The constructed vectors were transformed into *Escherichia coli* BL21(DE3) for the protein expression. The analyzed DNA sequences of recombinant *c-myc* and *max* were ATG GCT AGC ATG ACT GGT GGA CAG CAA ATG GGT CGC GGA TCC GAA TTC GGA TCC ACC ATG GGA AAT GTC AAG AGG CGA ACA CAC AAC GTC TTG GAG CGC CAG AGG AGG AAC GAG CTA AAA CGG AGC TTT TTT GCC CTG CGT GAC CAG ATC CCG GAG TTG GAA AAC AAT GAA AAG GCC CCC AAG GTA GTT ATC CTT AAA AAA GCC ACA GCA TAC ATC CTG TCC GTC CAA GCA GAG GAG CAA AAG CTC ATT TCT GAA GAG GAC TTG TTG CGG AAA CGA CGA GAA CAG TTG AAA CAC AAA CTT GAA CAG CTA CGG AAC TCT TGT GCG CTC GAG CAC CAC CAC CAC CAC CAC and ATG GCT AGC ATG ACT GGT GGA CAG CAA ATG GGT CGC GGA TCC ACC ATG GGA GAC AAA CGG GCT CAT CAT AAT GCA CTG GAA CGA AAA CGT AGG GAC CAC ATC AAA GAC AGC TTT CAC AGT TTG CGG GAC TCA GTC CCA TCA CTC CAA GGA GAG AAG GCA TCC CGG GCC CAA ATC CTA GAC AAA GCC ACA GAA TAT ATC CAG TAT ATG CGA AGG AAA AAC CAC ACA CAC CAG CAA GAT ATT GAC GAC CTC AAG CGG CAG AAT GCT CTT CTG GAG CAG CAA GTC CGT GCA CTG GAG AAG GCG AGG TCA CTC GAG CAC CAC CAC CAC CAC CAC, respectively. The protein sequences expected to be expressed are MASMT GGQQM GRGSE FGSTM GNVKR RTHNV LERQR RNELK RSFFA LRDQI PELEN NEKAP KVVIL KKATA YILSV QAEEQ KLISE EDLLR KRREQ LKHKL EQLRN SCALE HHHHH H and MASMT GGQQM GRGST MGDKR AHHNA LERKR RDHIK DSFHS LRDSV TSLQG EKASR AQILD KATEY IQYMR RKNHT HQQDI DDLKR QNALL EQQVR ALEKA RSLEH HHHHH, respectively. The underlined parts are homologous with human origins (Fig. 1).

Overexpression and purification of recombinant Max and c-Myc. Each colony containing recombinant human *c-myc* and *max* gene was grown in the LB culture media containing 0.1 mg ml^{-1} ampicillin at 37 °C until their OD_{600} reached 0.6. Following incubation with 1 mM IPTG for 7 hr, the cultures were harvested at 4 °C by ultracentrifuge. The harvested cells including recombinant Max protein were resuspended with Binding buffer solution (0.5 M NaCl, 20 mM Tris hydrochloride (pH 7.9), and 5 mM imidazole). Since recombinant Max proteins (Max85) were produced with a His-tag, they were purified easily with nickel-ion affinity chromatography (Novagen, Germany) at 4 °C. Final elute buffer solution contained 0.5 M NaCl, 20 mM Tris hydrochloride (pH 7.9), and 0.5 M imidazole. The harvested cells including recombinant c-Myc (Myc87) protein were resuspended with Binding buffer solution containing 6 M urea, 0.5 M NaCl, 20 mM Tris hydrochloride (pH 7.9), and 5 mM imidazole. Myc87 was purified with nickel-ion affinity chromatography at 4 °C. Final elute buffer solution contained 6 M urea, 0.5 M NaCl, 20 mM Tris hydrochloride (pH 7.9), and 0.5 M imidazole.

Preparation of protein stock solutions. Eluted buffer solutions containing Myc87 and Max85 were dialyzed into binding buffer solution, and each binding buffer solution containing purified Max85 and Myc87 was diluted and dialyzed into TBS (Tris-buffered saline; 137 mM NaCl, 2.68 mM KCl, and 10 mM Tris–HCl, pH adjusted to 7.4) and into PBS (phosphate-buffered saline; 137 mM NaCl, 2.68 mM KCl, 10.14 mM Na_2HPO_4, and 1.76 mM KH_2PO_4, pH adjusted to 7.4). The precipitate formed during dialysis was removed immediately by 0.20 μm syringe filter. The concentrations of Max85 and Myc87 dissolved in each buffer solution were determined spectrophotometrically, and the purity of

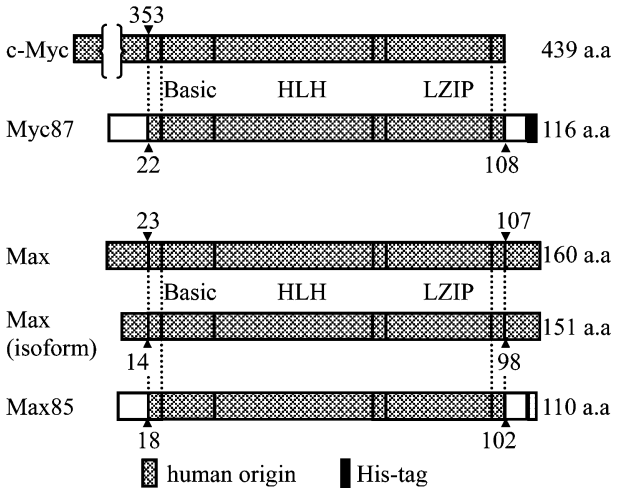

Fig. 1. Schematic diagram of Myc87 and Max85. A His-tag was attached to the C-terminal region of Myc87 and Max85. Eighty-seven amino acids (22–108) of Myc87 and 85 amino acids (18–102) of Max85 are homological with human c-Myc and Max, respectively. The sequences of the bHLHZip regions of Myc87 and Max85, which are the kernel in the formation of DNA/Myc/Max complexes, are identical with those of human origin.

proteins was determined by SDS–PAGE and image analysis software (TotalLab, NonLinear Dynamics, UK).

Western blot analysis. Purified Myc87, Max85, and Western size marker (West-view, Elips-Biotech, Korea) were electrophoresed in SDS–polyacrylamide gel. The separated proteins were electrotransferred from SDS–polyacrylamide gel to nitrocellulose membrane (ECL; Amersham) for 1 h at 250 mA. The nitrocellulose membrane with transferred proteins was then blocked with 5% skim milk in TBS-T (TBS, 0.1% Tween 20) overnight, and incubated with primary antibody (100 ng ml^{-1}) at room temperature for 1 h. The primary antibodies were mouse monoclonal IgG_1 antibody raised against a peptide corresponding to amino acids 408–439 within the C-terminal domain of c-Myc of human origin (Santa Cruz Biotechnology, CA) for Myc87 and rabbit monoclonal antibody raised against a recombinant protein corresponding to amino acids 28–151 representing the C-terminal domain of Max21 of human origin (Santa Cruz Biotechnology, CA) for Max85. The blots were washed four times with TBS-T, and incubated with HRP-conjugated anti-IgG antibody (Santa Cruz Biotechnology, CA) for 1 h. Immunoreactive bands were developed using ECL Western blotting detection reagents (Amersham Biosciences), and visualized on the film through exposure for 1 min.

Electrophoretic mobility shift assay. The proportions of protein–DNA complexes in each buffer solution were determined by measurement of the intensity of bands on an autoradiograph generated by electrophoretic mobility shift assay (EMSA). Myc–Max consensus oligonucleotides (5′-dGGAAGCAGACCACGTGGTCTGCTTCC-3′, Santa Cruz Biotechnology, US) were labeled using [γ-^{32}P]ATP and T4 polynucleotide kinase (TaKaRa bio, Japan). Protein mixtures were incubated at 37 °C for 10 min, and labeled DNA was added. In order to accomplish a state of equilibrium, we incubated the whole mixtures at 37 °C for 15 min. The protein–DNA complexes were separated from the free DNA on a 6% polyacrylamide gel prepared and pre-electrophoresed in the 0.5× TBE buffer (45 mM Tris–HCl, 45 mM boric acid, 10 mM EDTA (pH 8.0)). Electrophoresis was performed in the 0.5× TBE buffer at 100 V and 37 °C for 1 h. Each band was visualized by autoradiography, and the intensities of bands were measured by image analysis software (TotalLab, NonLinear Dynamics, UK).

Calculation of dissociation constant. The proposed mechanism of the formation of homodimer–DNA complex is

$$2A + DNA \leftrightarrow A_2 + DNA \leftrightarrow A_2 \cdot DNA \tag{1}$$

where A, A_2, and DNA denote the protein monomer, homodimer, and the consensus oligonucleotide, respectively. The dissociation constants in this reaction are

$$K_{d1} = \frac{[A]^2}{[A_2]}, \tag{2}$$

$$K_{d2} = \frac{[A_2] \times [D]}{[A_2D]}, \tag{3}$$

$$K_d = K_{d1} \times K_{d2} = \frac{[A]^2 \times [D]}{[A_2D]}, \tag{4}$$

$$[A]_0 = [A] + 2[A_2] + 2[A_2D],$$

$$[D]_0 = [D] + [A_2D],$$

where $[A]_0$, $[D]_0$, [D], and $[A_2D]$ are the initial concentration of A, the concentrations of total DNA, free DNA, and bound DNA, respectively. The dimer dissociation constant (K_{d1}) rearranges to

$$K_{d1} = \frac{([A]_0 - 2[A_2] - 2[A_2D])^2}{[A_2]},$$
$$4[A_2]^2 - (K_{d1} + 4[A]_0 - 8[A_2D])[A_2] + ([A_0]^2 + 4[A_2D]^2 - 4[A]_0[A_2D]) = 0. \tag{5}$$

In the experiments, the concentration of protein was much larger than that of DNA. So, concentration of homodimer is

$$[A_2] = \frac{K_{d1} + 4[A]_0 - \sqrt{(K_{d1} + 4[A]_0)^2 - 16[A]_0^2}}{8}. \tag{6}$$

The intensities of the bands on the autoradiograph are proportionate to the concentration of protein–DNA complexes, so the DNA-binding dissociation constant (K_{d2}) rearranges to

$$K_{d2} = \frac{[A_2][D]}{[A_2D]} = \frac{[A_2]([D]_0 - [A_2D])}{A_2D} = \frac{[A_2](M - I)}{I},$$
$$I = M\frac{[A_2]}{[A_2] + K_{d2}}, \tag{7}$$

where M and I denote the estimated maximum intensity, which can be found when all the DNA is bound by the dimeric protein, and the individual intensity according to the initial concentration of protein, respectively. Substitution of Eq. (6) in Eq. (7) gives

$$I = M\frac{\left(K_{d1} + 4[A]_0 - \sqrt{(K_{d1} + 4[A]_0)^2 - 16[A]_0^2}\right)/(8)}{\left(K_{d1} + 4[A]_0 - \sqrt{(K_{d1} + 4[A]_0)^2 - 16[A]_0^2}\right)/(8) + K_{d2}}. \tag{8}$$

The proposed mechanism of the formation of heterodimer–DNA complex is

$$A + B + DNA \leftrightarrow AB + DNA \leftrightarrow AB \cdot DNA, \tag{9}$$

where A, B, and AB denote protein monomer, another protein monomer and protein dimer, respectively. The dissociation constants in the formation of heterodimer–DNA complex are

$$K_{d1} = \frac{[A] \times [B]}{[AB]}, \tag{10}$$

$$K_{d2} = \frac{[AB] \times [D]}{[ABD]}, \tag{11}$$

$$K_d = K_{d1} \times K_{d2} = \frac{[A] \times [B] \times [D]}{[ABD]}, \tag{12}$$

$$[A]_0 = [A] + [AB] + [ABD],$$

$$[B]_0 = [B] + [AB] + [ABD],$$

$$[D]_0 = [D] + [ABD].$$

[AB] and [ABD] denote the concentration of heterodimer and that of heterodimer–DNA complex, respectively. The dimer dissociation constant (K_{d1}) rearranges to

$$K_{d1} = \frac{[A][B]}{[AB]} = \frac{([A]_0 - [AB] - [ABD])([B]_0 - [AB] - [ABD])}{[AB]},$$
$$[AB]^2 - (K_{d1} + [A]_0 + [B]_0 - 2[ABD])[AB] + [A]_0[B]_0 - [A]_0[ABD] - [B]_0[ABD] + [ABD]^2 = 0. \tag{13}$$

In the same way as in the formation of homodimer–DNA complex, the concentration of DNA was much lower than that of protein in this experiment, and the concentration of heterodimer is

$$[AB] = \frac{K_{d1} + [A]_0 + [B]_0 - \sqrt{(K_{d1} + [A]_0 + [B]_0)^2 - 4[A]_0[B]_0}}{2}. \tag{14}$$

So,the second dissociation constant can be rearranged to

$$K_{d2} = \frac{[AB][D]}{[ABD]} = \frac{[AB]([D]_0 - [ABD])}{[ABD]} = \frac{[AB](M - I)}{I},$$
$$I = M\frac{[AB]}{[AB] + K_{d2}}. \tag{15}$$

Substitution of Eq. (14) for [AB] in Eq. (15) gives

$$I = M\frac{\left(K_{d1} + [A]_0 + [B]_0 - \sqrt{(K_{d1} + [A]_0 + [B]_0)^2 - 4[A]_0[B]_0}\right)/(2)}{\left(K_{d1} + [A]_0 + [B]_0 - \sqrt{(K_{d1} + [A]_0 + [B]_0)^2 - 4[A]_0[B]_0}\right)/(2) + K_{d2}}. \quad (16)$$

We drew the plots of individual intensity against the initial concentration of protein. With substituting the individual intensity corresponding to the initial concentration of protein in Eq. (8) and Eq. (16), we plotted the regression curves fitting the experimental results, and determined the maximum intensity and the dissociation constants.

Results and discussion

Recombinant c-Myc and Max proteins

Recombinant c-Myc (Myc87) and Max (Max85) were expressed in *Escherichia coli* (*E. coli*) BL21 and were purified. The calculated molecular weights of Myc87 and Max85 are 13589.53 and 12865.37, respectively (http://us.expasy.org). The molecular weights measured by MALDI-TOF were 13353.97 for Myc87, and 12768.02 for Max85. The apparent molecular weights of Myc87 and Max85 on SDS–PAGE were about 16 kDa, and this reflects the anomalous electrophoretic mobility typical for recombinant c-Myc and Max. The purities of Myc87 and Max85 determined by SDS–PAGE and image analysis software (TotalLab, NonLinear Dynamics, UK) were 92.6% for Myc87 and 98.9% for Max85. These purities were applied to determine the concentration of recombinant proteins. The homology of Myc87 and Max85 with human origin was verified by monoclonal antibodies (Fig. 2).

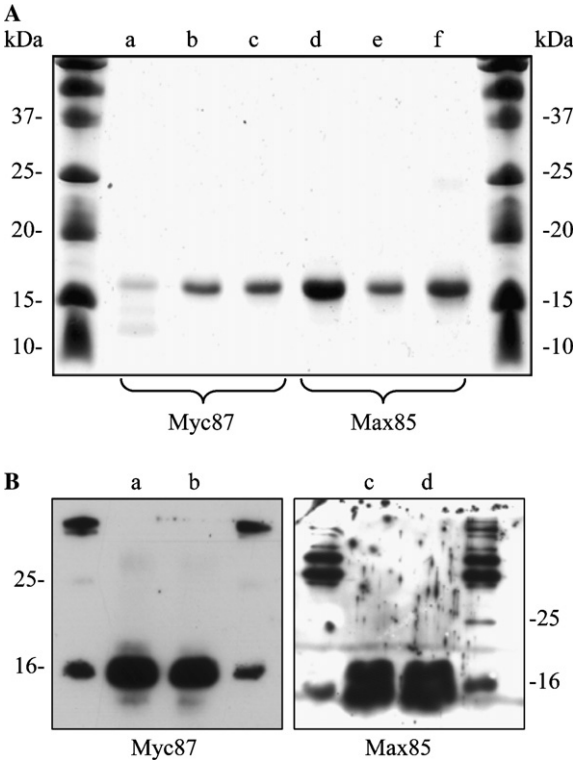

Fig. 2. Overexpression and purification of Myc87 and Max85. (A) Myc87 and Max85 were harvested in each other buffer solution and purified with nickel-ion affinity chromatography. Lanes a and d, purified Myc87 and Max85 which were dissolved in binding buffer; lanes b and e, purified Myc87 and Max85 which were extracted from inclusion body in binding buffer; lanes c and f, purified Myc87 and Max85 which were dissolved in binding buffer including 6 M urea. (B) Western blotting analysis of purified Myc87 and Max85; the size marker proteins cross-reacted with the antibodies. Lanes a and c, proteins dissolved in TBS; lanes b and d, proteins dissolved in PBS.

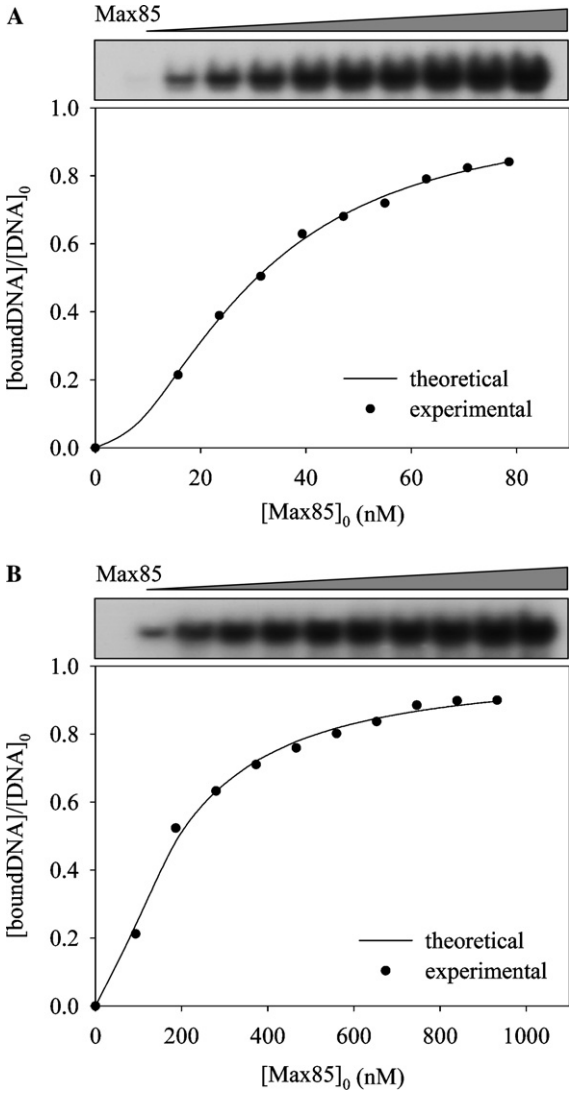

Fig. 3. Proportions of Max85/Max85/DNA in TBS and in PBS. Proportion of bound DNA to total DNA plotted versus the initial concentration of Max85. Data expressed as dots are experimental results and the regression curve is plotted as a line. (A) Proportion of bound DNA in TBS. The concentration of DNA was 89.8 pM and each sample contains 137 mM NaCl, 2.68 mM KCl, and 10 mM Tris–HCl (pH adjusted to 7.4). The initial concentrations of Max85 were 15.7, 23.6, 31.4, 39.3, 47.1, 55.0, 62.8, 70.7, and 78.5 nM. (B) Proportion of bound DNA in PBS. The concentration of DNA was 89.8 pM and each sample contains 137 mM NaCl, 2.68 mM KCl, 10.14 mM Na_2HPO_4, and 1.76 mM KH_2PO_4 (pH adjusted to 7.4). The initial concentrations of Max85 were 93.3, 187, 280, 373, 466, 560, 653, 746, 839, and 933 nM.

Unfortunately, the concentration of the recombinant proteins dissolved in each buffer solution was under 20 μg ml^{-1}, so we could not check the native structure by the circular dichroism spectroscopy. But, the precipitate formed during dialysis was removed immediately, therefore we were convinced that most proteins preserve their property of dimerization and DNA-binding.

Analyses of Max85/Max85/DNA and Myc87/Myc87/DNA complexes

The protein–DNA complexes were composed in TBS and in PBS, which are the most common buffer solutions. The determined K_{d1}, K_{d2}, and K_d are $5.90(\pm0.54)\times10^{-7}$ M, $1.33(\pm0.21)\times10^{-9}$ M, and $7.83(\pm0.53)\times10^{-16}$ M^2 in TBS, and are $5.61(\pm0.34)\times10^{-7}$ M, $3.12(\pm0.79)\times10^{-8}$ M, and $1.75(\pm0.34)\times10^{-14}$ M^2 in PBS. Compared with the dissociation constants in TBS, the value of K_{d2} in PBS increases considerably. This result means that the affinity of Max85 homodimer for DNA in TBS is stronger than that in PBS (Fig. 3).

Myc proteins also homodimerized and bound the DNA, but the amount of Myc homodimer/DNA complex was a small quantity compared with that of Max homodimer/DNA complex. The values of K_{d1}, K_{d2}, and K_d determined for Myc87 homodimer/DNA complex in TBS are $6.85(\pm0.25)\times10^{-3}$ M, $2.27(\pm0.08)\times10^{-12}$ M, and $1.55(\pm0.11)\times10^{-14}$ M^2, respectively. Compared with Max85 homodimer/DNA complex in TBS, the first dissociation constant is reduced considerably. From this experimental result, a small quantity of Myc homodimer/DNA is considered to be caused by the weak affinity between Myc proteins. On the contrary, the second dissociation constant is larger than that of Max85 in TBS. and this result means that the sequence-specific affinity of Myc protein is stronger than that of Max protein. The experiment to verify the formation of Myc87 homodimer/DNA complex could not be performed in PBS. The proportion of Myc87/Myc87/DNA in PBS complex was not detectable in the range of these concentrations. K_d in the formation of Myc87/Myc87/DNA in PBS is considered to be much larger than that in TBS (Fig. 4).

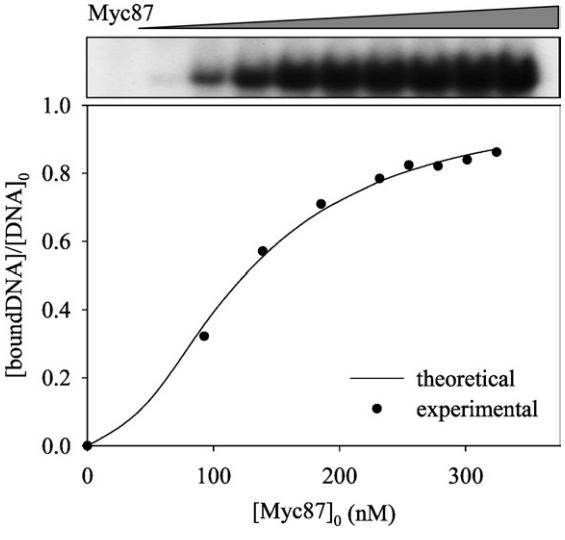

Fig. 4. Proportions of Myc87/Myc87/DNA in TBS. Proportion of Myc87/Myc87/DNA to total DNA in TBS plotted versus the initial concentration of Myc87. Data expressed as dots are experimental results and the regression curve is plotted as a line. The concentration of DNA was 89.8 pM. The initial concentrations of Myc87 were 92.7, 139, 185, 232, 255, 278, 301, and 324 nM.

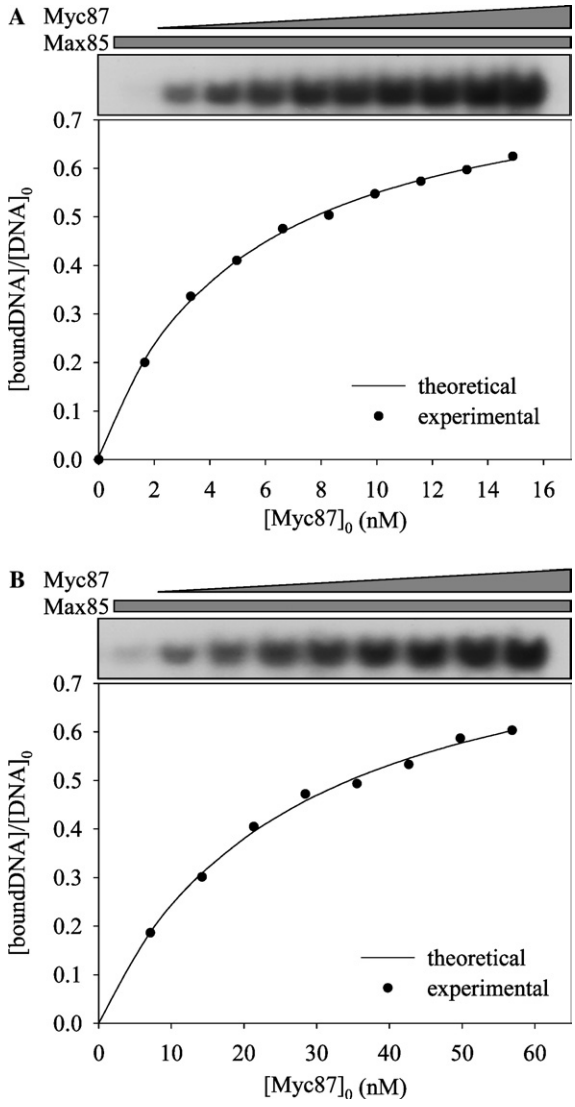

Fig. 5. Proportions of Myc87/Max85/DNA in TBS and in PBS. Proportion of bound DNA to total DNA in TBS plotted versus the initial concentration of Myc87. Data expressed as dots are experimental results and the regression curve is plotted as a line. (A) Proportion of bound DNA in TBS. Concentrations of DNA and Max85 were 89.8 pM and 2.00 nM in all samples, respectively. The initial concentrations of Myc87 were 1.66, 3.31, 4.97, 6.62, 8.28, 9.93, 11.6, 13.2, and 14.9 nM. (B) Proportion of bound DNA in PBS. Concentrations of DNA and Max85 were 89.8 pM and 13.7 nM in all samples, respectively. The initial concentrations of Myc87 were 7.11, 14.2, 21.3, 28.4, 35.5, 42.6, 49.7, and 56.9 nM.

Table 1
Determined dissociation constants

	Max85/Max85/DNA		Myc87/Myc87/DNA	Myc87/Max85/DNA	
	TBS	PBS	TBS	TBS	PBS
K_{d1} (M)	$5.90(\pm0.54)\times10^{-7}$	$5.61(\pm0.34)\times10^{-7}$	$6.85(\pm0.25)\times10^{-3}$	$2.55(\pm0.29)\times10^{-8}$	$1.98(\pm0.71)\times10^{-7}$
K_{d2} (M)	$1.33(\pm0.21)\times10^{-9}$	$3.12(\pm0.79)\times10^{-8}$	$2.27(\pm0.08)\times10^{-12}$	$4.43(\pm0.37)\times10^{-10}$	$1.94(\pm0.57)\times10^{-9}$
K_d (M^2)	$7.83(\pm0.53)\times10^{-16}$	$1.75(\pm0.34)\times10^{-14}$	$1.55(\pm0.11)\times10^{-14}$	$1.13(\pm0.22)\times10^{-17}$	$3.83(\pm2.51)\times10^{-16}$

Analysis of Myc87/Max85/DNA complexes

We determined the dissociation constants in the formation of Myc87/Max85/DNA complex in TBS and PBS and compared each with the corresponding value obtained in the formation of Max85/Max85/DNA complex. A relatively small quantity of Max85 protein was mixed with Myc87 to reduce the formation of Max85/Max85/DNA complex to the extent of being negligible. To determine the dissociation constants in TBS, Max85 was diluted until the final concentration was 2.00 nM in TBS, with a final DNA concentration of 89.8 pM. Myc was added to this mixture and the final concentration was between 1.66 and 14.9 nM. We measured the intensities of bands on an autoradiograph and plotted the regression curve. The values of K_{d1}, K_{d2}, and K_d in TBS were $2.55(\pm0.29)\times10^{-8}$ M, $4.43(\pm0.37)\times10^{-10}$ M, and $1.13(\pm0.22)\times10^{-17}$ M^2, respectively. The final concentrations of Max85 and DNA in PBS were fixed at 13.7 nM and 89.8 pM, respectively, and the concentrations of Myc87 were between 7.11 and 64.0 nM. The values of K_{d1}, K_{d2}, and K_d determined in PBS are $1.98(\pm0.71)\times10^{-7}$ M, $1.94(\pm0.57)\times10^{-9}$ M, and $3.83(\pm2.51)\times10^{-16}$ M^2, respectively (Fig. 5).

Compared with the dissociation constants in the formation of Max homodimer/DNA complex, K_{d1} and K_{d2} are reduced considerably. This result means that the affinity between Myc87 and Max85 is much stronger than that between Max85 and Max85, and that the affinity of heterodimer for DNA is increased compared with that of Max homodimer. According to former studies, most of the E-box sites are occupied by Myc/Max heterodimer rather than by Max homodimer or by Myc homodimer. This result may be caused by the disparity in respective dissociation constants between homodimer–DNA complex and heterodimer–DNA complex (Table 1).

Effects of inhibitor for Max85/Max85/DNA complex

Some kinds of unsaturated fatty acid, such as linoleic acid and arachidonic acid [20], are known to inhibit the formation of Max/Max/DNA complex. We added linoleic acid to the mixture composed with Max85 and DNA to confirm which step is affected by linoleic acid. The final concentration of Max85 was set between 30.22 and 302.2 nM, and then linoleic acid was added at the concentration of 50 μM. The K_{d1}, K_{d2}, and K_d determined in this experiment are $2.22(\pm0.07)\times10^{-7}$ M, $2.03(\pm0.34)\times10^{-8}$ M, and $4.50(\pm0.63)\times10^{-15}$ M^2, respectively. Compared with the dissociation constants from the formation of Max85 homodimer/DNA complex in TBS, K_{d1} is reduced slightly, but K_{d2} is increased about 15 times. With considering the decrease of the affinity of dimer for DNA, we concluded that some kinds of unsaturated fatty acid block the DNA-binding site, and reduce the affinity of dimer for DNA (Fig. 6).

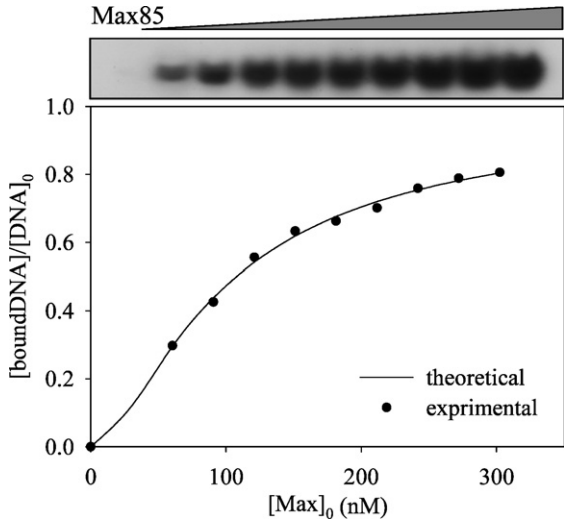

Fig. 6. Proportions of Max85/Max85/DNA in TBS containing linoleic acid. Proportion of Max85/Max85/DNA to total DNA in TBS containing linoleic acid plotted versus the initial concentration of Max85. Each sample contains 137 mM NaCl, 2.68 mM KCl, 50 μM linoleic acid, and 10 mM Tris–HCl (adjusted pH to 7.4). Concentration of DNA was 89.8 pM in each sample, and the initial concentrations of Max85 were 60.4, 90.7, 121, 151, 181, 212, 242, 272, and 302 nM.

Acknowledgments

Financial support in part from the Brain Korea 21 program is gratefully acknowledged. Mr. Kyung Chae Jung, Ho Sung Rhee, and Chi Hoon Park thank the Ministry of Education for the Brain Korea 21 fellowship.

References

[1] C.V. Dang, L.M. Resar, E. Emison, S. Kim, Q. Li, J.E. Prescott, D. Wonsey, K. Zeller, Function of the c-Myc oncogenic transcription factor, Exp. Cell Res. 253 (1999) 63–77.

[2] L.M. Facchini, L.Z. Penn, The molecular role of Myc in growth and transformation: recent discoveries lead to new insights, FASEB J. 12 (1998) 633–651.

[3] M. Eilers, Control of cell proliferation by Myc family genes, Mol. Cells 9 (1999) 1–6.

[4] E.M. Blackwood, R.N. Eisenman, Max: a helix–loop–helix zipper protein that forms a sequence-specific DNA-binding complex with Myc, Science 251 (1991) 1211–1217.

[5] G.C. Prendergast, D. Lawe, E.B. Ziff, Association of Myn, the murine homolog of max, with c-Myc stimulates methylation-sensitive DNA binding and ras cotransformation, Cell 65 (1991) 395–407.

[6] E.M. Blackwood, B. Luscher, R.N. Eisenman, Myc and Max associate in vivo, Genes Dev. 6 (1992) 71–80.

[7] A. Wenzel, C. Cziepluch, U. Hamann, J. Schurmann, M. Schwab, The N-Myc oncoprotein is associated in vivo with the phosphoprotein Max(p20/22) in human neuroblastoma cells, EMBO J. 10 (1991) 3703–3712.

[8] T.K. Blackwell, L. Kretzner, E.M. Blackwood, R.N. Eisenman, H. Weintraub, Sequence-specific DNA binding by the c-Myc protein, Science 250 (1990) 1149–1151.

[9] E. Kerkhoff, K. Bister, K.H. Klempnauer, Sequence-specific DNA binding by Myc proteins, Proc. Natl. Acad. Sci. USA 88 (1991) 4323–4327.

[10] B. Amati, T.D. Littlewood, G.I. Evan, H. Land, The c-Myc protein induces cell cycle progression and apoptosis through dimerization with Max, EMBO J. 12 (1993) 5083–5087.

[11] M. Guerin, M. Barrois, M.J. Terrier, M. Spielmann, G. Riou, Overexpression of either c-myc or c-erbB-2/neu proto-oncogenes in human breast carcinomas: correlation with poor prognosis, Oncogene Res. 3 (1988) 21–31.

[12] R. Mariani-Costantini, C. Escot, C. Theillet, A. Gentile, G. Merlo, R. Lidereau, R. Callahan, In situ c-myc expression and genomic status of the c-myc locus in infiltrating ductal carcinomas of the breast, Cancer Res. 48 (1988) 199–205.

[13] D.A. Spandidos, J.K. Field, N.J. Agnantis, G.I. Evan, J.P. Moore, High levels of c-myc protein in human breast tumours determined by a sensitive ELISA technique, Anticancer Res. 9 (1989) 821–826.

[14] L. Kretzner, E.M. Blackwood, R.N. Eisenman, Myc and Max proteins possess distinct transcriptional activities, Nature 359 (1992) 426–429.

[15] C. Escot, J. Simony-Lafontaine, T. Maudelonde, C. Puech, H. Pujol, H. Rochefort, Potential value of increased MYC but not ERBB2 RNA levels as a marker of high-risk mastopathies, Oncogene. 8 (1993) 969–974.

[16] M. Shibuya, J. Yokota, Y. Ueyama, Amplification and expression of a cellular oncogene (c-myc) in human gastric adenocarcinoma cells, Mol. Cell. Biol. 5 (1985) 414–418.

[17] A.R. Ferre-D'Amare, G.C. Prendergast, E.B. Ziff, S.K. Burley, Recognition by Max of its cognate DNA through a dimeric b/HLH/Z domain, Nature 363 (1993) 38–45.

[18] S.K. Nair, S.K. Burley, X-ray structures of Myc–Max and Mad–Max recognizing DNA. Molecular bases of regulation by proto-oncogenic transcription factors, Cell 112 (2003) 193–205.

[19] W. Fieber, M.L. Schneider, T. Matt, B. Krautler, R. Konrat, K. Bister, Structure, function, and dynamics of the dimerization and DNA-binding domain of oncogenic transcription factor v-Myc, J. Mol. Biol. 307 (2001) 1395–1410.

[20] S. Chung, S. Park, C.H. Yang, Unsaturated fatty acids bind Myc–Max transcription factor and inhibit Myc–Max–DNA complex formation, Cancer Lett. 188 (2002) 153–162.